

## Multicolor fluorescence enhancement from a photonics crystal surface

A. Pokhriyal,<sup>1</sup> M. Lu,<sup>2</sup> C. S. Huang,<sup>3</sup> S. Schulz,<sup>2</sup> and B. T. Cunningham<sup>3,a)</sup>

<sup>1</sup>*Department of Physics, University of Illinois at Urbana-Champaign, 1110 W. Green Street, Urbana, Illinois 61801, USA*

<sup>2</sup>*SRU Biosystems, 14-A Gill Street, Woburn, Massachusetts 01801, USA*

<sup>3</sup>*Department of Electrical and Computer Engineering, University of Illinois at Urbana-Champaign, 1406 W. Green Street, Urbana, Illinois 61801, USA*

(Received 12 July 2010; accepted 11 August 2010; published online 24 September 2010)

A photonic crystal substrate exhibiting resonant enhancement of multiple fluorophores has been demonstrated. The device, fabricated uniformly from plastic materials over a  $\sim 3 \times 5$  in.<sup>2</sup> surface area by nanoreplica molding, utilizes two distinct resonant modes to enhance electric field stimulation of a dye excited by a  $\lambda = 632.8$  nm laser (cyanine-5) and a dye excited by a  $\lambda = 532$  nm laser (cyanine-3). Resonant coupling of the laser excitation to the photonic crystal surface is obtained for each wavelength at a distinct incident angle. Compared to detection of a dye-labeled protein on an ordinary glass surface, the photonic crystal surface exhibited a  $32\times$  increase in fluorescent signal intensity for cyanine-5 conjugated streptavidin labeling, while a  $25\times$  increase was obtained for cyanine-3 conjugated streptavidin labeling. The photonic crystal is capable of amplifying the output of any fluorescent dye with an excitation wavelength in the  $532 \text{ nm} < \lambda < 633$  nm range by selection of an appropriate incident angle. The device is designed for biological assays that utilize multiple fluorescent dyes within a single imaged area, such as gene expression microarrays. © 2010 American Institute of Physics. [doi:10.1063/1.3485672]

Fluorescence is one of the most sensitive detection and imaging tools available for life science research and diagnostic assays,<sup>1</sup> representing the most common method for determining the presence and concentration of analytes in a wide range of applications including DNA sequencing, DNA microarrays, immunoassays, and cell imaging. The ability to detect weak signals is essential for assays requiring the detection of analytes at low concentration. To address this challenge, researchers have developed many methods to enhance fluorescence emission, thereby improving detection sensitivity. A variety of nanopatterned surfaces have been studied for the purpose of enhancing fluorescence output.<sup>2–6</sup> Field enhancement in these structures arises from several effects which include locally intense optical fields, reduced fluorescence lifetimes, and directional emission.<sup>7–10</sup>

Photonic crystal (PC) surfaces comprised of a periodic surface grating coated with a high refractive index dielectric have been demonstrated for fluorescence emission enhancement applications<sup>11</sup> through the use of narrowband resonant modes at specific wavelengths. PC-enhanced fluorescence (PCEF) takes advantage of the resonant evanescent field that has an increased local energy density compared to the excitation light source. The intensified evanescent field strongly excites fluorophores located within an evanescent decay length of the sensor surface, resulting in enhanced emission. Previous publications have demonstrated the use of PCEF with the resonant mode spectrally overlapping the laser wavelength, to excite fluorescent dyes,<sup>12</sup> and, at normal incidence illumination, a PC with a resonant mode at  $\lambda = 632.8$  nm producing a 60-fold magnification of cyanine-5 (Cy-5) signal compared to an ordinary glass substrate.<sup>13</sup>

Many biological fluorescence assays, such as gene expression microarrays,<sup>14,15</sup> have been developed using multiple fluorescent dyes within a single imaged area. In order to

enhance the emission from multiple fluorescent dyes, the PC surface must be designed with resonant wavelengths coinciding with the wavelength of multiple lasers that are used to excite the target fluorophores. The PC structure intrinsically supports resonant modes in a wavelength range as wide as 200 nm,<sup>16</sup> because each wavelength couples resonantly with the structure for a distinct angle of incidence. Therefore, by designing a PC that can resonantly couple light from multiple excitation lasers each at a distinct incident angle, it is possible to provide enhanced fluorescence for multiple dyes. The fluorescent images of each dye can then be taken using a multilaser confocal scanning detection instrument which has the ability to excite the PC surface with a selected angle of incidence, and the wavelength/angle combination that yields PCEF. In this report, we describe the design and characterization of a PC surface that is used to enhance the fluorescence from Cy-5 (excited by a  $\lambda = 632.8$  HeNe laser) and Cy-3 (excited by a  $\lambda = 532$  nm diode pumped solid state laser).

A cross-sectional diagram (not to scale) of the PC surface is shown in Fig. 1. The one-dimensional (1D) surface grating structure was formed in ultraviolet curable polymer (UVCP) on a polyethylene-terephthalate (PET) substrate by the nanoreplica molding technique.<sup>17</sup> The polymer grating surface was coated with a high refractive index dielectric layer of TiO<sub>2</sub> which functions as a wave confinement layer. Under broadband illumination, a highly efficient reflection represents a resonance at a specific wavelength and a specific angle. A simulation tool (DiffractMOD, RSoft Design Group) based on the rigorous coupled-wave analysis (RCWA) technique was used to design the 1D surface PC structure. In order to support resonances at  $\lambda = 632.8$  and 532 nm concurrently, RCWA simulation results stipulated the use of a grating with a period of  $\Lambda = 360$  nm. Other device parameters include the grating depth of  $d = 25$  nm, TiO<sub>2</sub> thickness of  $t_{\text{TiO}_2} = 120$  nm, UVCP refractive index of  $n_{\text{UVCP}}$

<sup>a)</sup>Electronic mail: bcunning@illinois.edu.

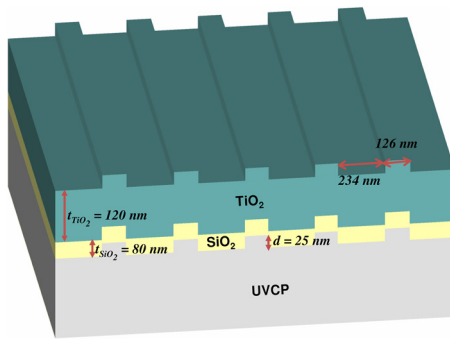


FIG. 1. (Color online) Cross-sectional diagram (not to scale) of the PC. The dimensions are as follows:  $\Lambda=360$  nm, grating depth  $d=25$  nm,  $\text{SiO}_2$  thickness  $t_{\text{SiO}_2}=80$  nm, and  $\text{TiO}_2$  thickness  $t_{\text{TiO}_2}=120$  nm. The grating width is 35% of the period.

$=1.47$ , and  $\text{TiO}_2$  refractive index of  $n_{\text{TiO}_2}=2.35$ . The transmission spectra were calculated by RCWA and the minimum transmissions (or maximum reflections) in the spectra were used to identify the resonant mode supported by the designed structure.<sup>18</sup> As shown in Fig. 2, a photonic band diagram for the structure shown in Fig. 1 was calculated for transverse magnetic (TM) modes in the  $510 \text{ nm} < \lambda < 660 \text{ nm}$  wavelength interval where the incident angle varied from  $0^\circ < \theta < 20^\circ$ . From the photonic band diagram, a resonant angle of  $\theta=13.8^\circ$  corresponds to a resonant wavelength of  $\lambda=532 \text{ nm}$ , while a resonant angle of  $\theta=9.2^\circ$  corresponds to a resonant wavelength of  $\lambda=632.8 \text{ nm}$ . Figure 3 shows the spatial distribution of the simulated near-field electric field intensity (normalized to the intensity of incident field) for the excitation of the resonant mode at  $\lambda=532$  and  $632.8 \text{ nm}$ . The influence of the resonance phenomenon on the resulting near-fields is clearly manifested in the electric field intensity.

Fabrication of the device was carried out using a plastic-based nanoreplica molding process. Briefly, a silicon wafer with a negative surface volume image of the desired grating pattern was fabricated using deep-UV lithography and reactive ion etching. A liquid UVCP was sandwiched between a PET sheet and the silicon master wafer, and was subsequently cured using a high intensity UV lamp (Xenon, Inc.). The hardened polymer grating adhered to the PET and was peeled away from the master, and the replica was cut and attached to a  $1 \times 3 \text{ in.}^2$  microscope slide. A thin  $\text{SiO}_2$  intermediate layer ( $t_{\text{SiO}_2}=80 \text{ nm}$ ) on the grating surface helps to reduce autofluorescence background from the underlying polymer material. Following  $\text{SiO}_2$  deposition, 120 nm of

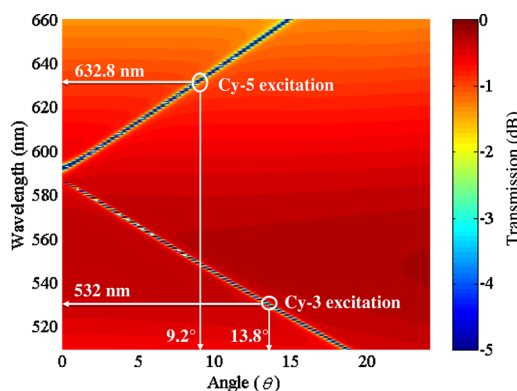


FIG. 2. (Color online) Simulated dispersion diagram for the PC used in this study by RCWA. Resonance for the enhanced excitation for the TM mode is  $\theta \sim 9.2^\circ$  for Cy-5 excitation and  $\theta \sim 13.8^\circ$  for Cy-3 excitation.

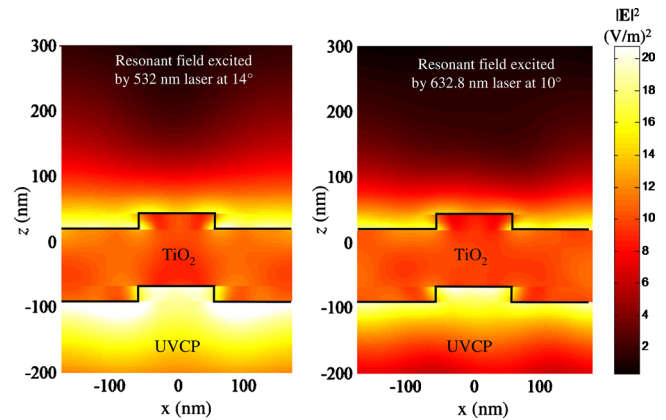


FIG. 3. (Color online) Simulated near field distribution for the PC used in this study by RCWA at  $\lambda=532 \text{ nm}$  and  $\lambda=633 \text{ nm}$ .

$\text{TiO}_2$  was sputtered by an rf sputtering system (PVD 75, Kurt Lesker). The photonic band diagram of the device was obtained by illuminating the device with collimated white light and measuring the transmitted spectrum with a spectrometer (USB 2000, Ocean Optics) as a function of incident angle. The consequent band diagram is shown in Fig. 4, which agrees well with the simulated band diagram shown in Fig. 2. As highlighted in Fig. 4, resonances for  $\lambda=532 \text{ nm}$  and  $\lambda=632.8 \text{ nm}$  modes lie at  $\theta=15^\circ$  and  $\theta=9^\circ$ , respectively.

In order to demonstrate the fluorescence enhancement performance of the fabricated sensor, a detection experiment using a dye-labeled protein was carried out on the PC surface and a reference glass slide. Both the PC surface and the glass slide were pre-cleaned with  $\text{O}_2$  plasma (TI Plasma) for 3 min. and functionalized by overnight incubation in an enclosed glass container with 5% 3-glycidoxypropyldimethylethoxysilane in dry toluene at  $100^\circ \text{C}$ . After incubation the silanized devices were cleaned by sonication in toluene, methanol and deionized (DI) water and then dried under a nitrogen stream. Cy-5 and Cy-3 conjugated streptavidin (GE Healthcare) at  $50 \mu\text{g/ml}$  was spotted onto the slides as two separate arrays by a piezodispenser (Piezorray, Perkin Elmer). After overnight incubation, the devices were washed by gently dipping them in a protein blocking buffer (Phosphate buffered saline at  $\text{pH} 7.4$  with Kathon antimicrobial agent) solution for 60 s. followed by DI water rinse. Fluorescent images of the spots were obtained using a commercially available confocal laser scanner (LS-Reloaded, Tecan) equipped with a  $\lambda=632.8 \text{ nm}$  He-Ne

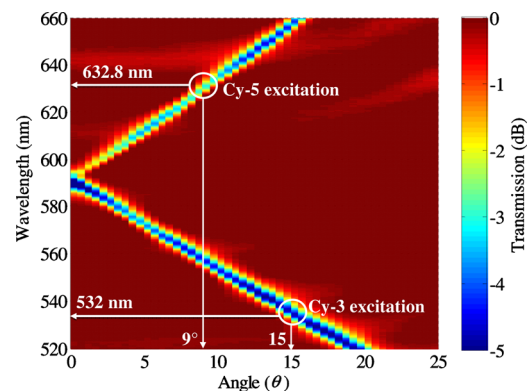


FIG. 4. (Color online) Measured dispersion diagram for the PC used in this study by RCWA for the enhanced excitation for the TM mode is  $\theta \sim 9^\circ$  for Cy-5 excitation and  $\theta \sim 15^\circ$  for Cy-3 excitation.

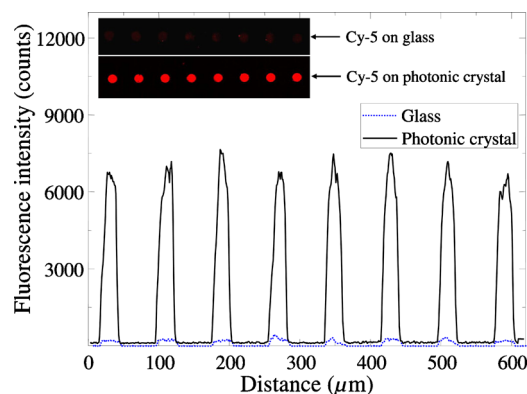


FIG. 5. (Color online) Intensity profile as a function of distance for a line of fluorescent image pixels profiling spots of Cy-5 conjugated streptavidin for both the glass slide and the PC under normal incidence illumination. The scanned images are shown in insets.

laser and a  $\lambda=532$  nm diode pumped solid state laser. The angle of incidence of both lasers can be tuned from  $\theta=0^\circ$  to  $\theta=25^\circ$ . The Cy-5 conjugated streptavidin and Cy-3 conjugated streptavidin spots were sequentially illuminated by TM-polarized  $\lambda=632.8$  nm and  $\lambda=532$  nm lasers with Cy-5 and Cy-3 emission filters ( $\lambda=692 \pm 20$  nm;  $\lambda=575 \pm 25$  nm). The measured images were analyzed by image processing software (ImageJ). The net fluorescence intensity was calculated by averaging spot intensities over the 16 replicate spots minus the local background intensity.

The He-Ne laser at  $\theta=15^\circ$  was used to excite the Cy-5 conjugated streptavidin spots, which demonstrated an amplification of Cy-5 emission on the PC surface by a factor of 32 compared to the glass slides measured under same condition. Similarly, Cy-3 conjugated streptavidin spots were excited by the green laser at  $\theta=9^\circ$ , which showed an enhancement by a factor of 25, compared to the glass surface. The scanned images from the PC and glass substrates are compared in the insets of Figs. 5 and 6 (images were plotted using the same color scale). Representative line profiles generated by extracting fluorescence intensities from a single line of pixels through eight spots on the PC and glass images for both fluorophores is also shown in Figs. 5 and 6. This profile clearly illustrates amplification of the emission signal from both fluorophores on the PC surface. The slight increase in background fluorescence in these images can be attributed to simultaneous enhancement of the fluorescent output originat-

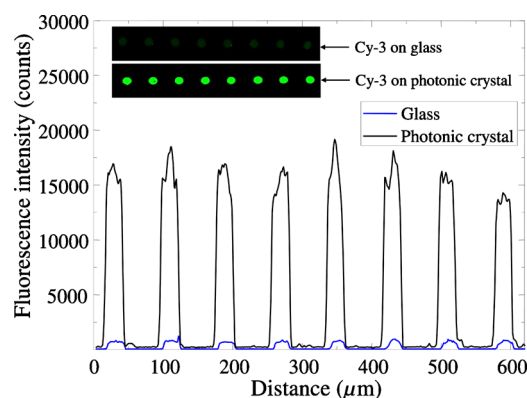


FIG. 6. (Color online) Intensity profile as a function of distance for a line of fluorescent image pixels profiling spots of Cy-3 conjugated streptavidin for both the glass slide and the PC under normal incidence illumination. The scanned images are shown in insets.

ing from the polymer material used for nanoreplica molding the grating structure. The fluorescence images of the spots were taken at the small pinhole setting in the confocal laser scanner (LS-Reloaded, Tecan) with  $10 \times 10 \mu\text{m}^2$  pixel resolution. A photomultiplier tube (PMT) gain of 100 was used to scan SA-conjugated Cy-3 spots and a PMT gain of 130 was used to scan SA-conjugated Cy-5 spots.

In summary, a single PC surface has been used to enhance fluorescence emission from both Cy-5 and Cy-3 dyes. The PC was fabricated by a low cost replica molding method that can be performed uniformly over a large surface area. To excite resonant modes at a desired wavelength, the excitation light needs to illuminate the PC at a specific resonant angle by tuning the angle of incidence of the detection instrument. For the device demonstrated here, the resonance angle for  $\lambda=632.8$  nm is  $\theta=9^\circ$  while for  $\lambda=532$  nm,  $\theta=15^\circ$ . Compared to a glass slide, the PC sensor exhibits an enhancement of  $32\times$  for Cy-5 and  $25\times$  for Cy-3. This particular PC is capable of PCEF for the wavelength range  $532 \text{ nm} < \lambda < 633$  nm, providing compatibility with a large variety of commonly used fluorescent dyes, such as Rhodamine, Texas Red, and Alexa fluor 532 to 647, which are widely used in life science research, diagnostic testing, and environmental detection.

This work was supported by National Institutes of Health (Grant No. GM086382A), the National Science Foundation (Grant No. CBET 07-54122), and SRU Biosystems. Any opinions, findings, conclusions, or recommendations expressed in this material are those of the authors and do not necessarily reflect the views of National Institutes of Health or the National Science Foundation. The authors thank the staff at the Micro and Nanotechnology Laboratory at the University of Illinois at Urbana-Champaign. Authors A. Pokhriyal and M. Lu contribute equally to the paper.

- <sup>1</sup>J. R. Lakowicz, *Principles of Fluorescence Spectroscopy*, 3rd ed. (Springer, New York, 2006), p. 954.
- <sup>2</sup>H.-Y. Wu, W. Zhang, P. C. Mathias, and B. T. Cunningham, *Nanotechnology* **21**, 7 (2010).
- <sup>3</sup>C. D. Geddes and J. R. Lakowicz, *J. Fluoresc.* **12**, 121 (2002).
- <sup>4</sup>E. Le Moal, E. Fort, S. Leveque-Fort, F. P. Cordelieres, M.-P. Fontaine-Aupart, and C. Ricolleau, *Biophys. J.* **92**, 2150 (2007).
- <sup>5</sup>L. C. Estrada, O. E. Martinez, M. Brunstein, S. Bouchoule, L. Le-Gratiet, A. Talneau, I. Sagnes, P. Monnier, J. A. Lvenson, and A. M. Yacomotti, *Opt. Express* **18**, 3693 (2010).
- <sup>6</sup>A. Kinkhabwala, Z. Yu, S. Fan, Y. Avlasevich, K. Müllen, and W. E. Moerner, *Nat. Photonics* **3**, 654 (2009).
- <sup>7</sup>J. R. Lakowicz, *Anal. Biochem.* **298**, 1 (2001).
- <sup>8</sup>S. Fan and J. D. Joannopoulos, *Phys. Rev. B* **65**, 235112 (2002).
- <sup>9</sup>K. A. Willets and R. P. Van Duyne, *Annu. Rev. Phys. Chem.* **58**, 30 (2006).
- <sup>10</sup>P. Anger, P. Bharadwaj, and L. Novotny, *Phys. Rev. Lett.* **96**, 113002 (2006).
- <sup>11</sup>N. Ganesh, I. D. Block, P. C. Mathias, W. Zhang, V. Malyarchuk, and B. T. Cunningham, *Opt. Express* **16**, 21626 (2008).
- <sup>12</sup>P. C. Mathias, N. Ganesh, W. Zhang, and B. T. Cunningham, *J. Appl. Phys.* **103**, 094320 (2008).
- <sup>13</sup>P. C. Mathias, H.-Y. Wu, and B. T. Cunningham, *Appl. Phys. Lett.* **95**, 021111 (2009).
- <sup>14</sup>W. Budach, D. Neuschaefer, C. Wanke, and S.-D. Chibout, *Anal. Chem.* **75**, 2571 (2003).
- <sup>15</sup>D. Che, Y. Bao, and U. R. Mueller, *J. Biomed. Opt.* **6**, 450 (2001).
- <sup>16</sup>N. Ganesh and B. T. Cunningham, *Appl. Phys. Lett.* **88**, 071110 (2006).
- <sup>17</sup>I. D. Block, L. L. Chan, and B. T. Cunningham, *Microelectron. Eng.* **84**, 603 (2007).
- <sup>18</sup>N. Ganesh, W. Zhang, P. C. Mathias, E. Chow, J. A. N. T. Soares, V. Malyarchuk, A. D. Smith, and B. T. Cunningham, *Nat. Nanotechnol.* **2**, 515 (2007).